Molecular Therapy
Nucleic Acids
Original Article

Chemically modified *in-vitro*-transcribed mRNA encoding thrombopoietin stimulates thrombopoiesis in mice

Yu Zhang,[1] Xiaodong Xi,[2] Hang Yu,[3] Liuyan Yang,[4] Jinzhong Lin,[5] Wen Yang,[1] Junling Liu,[1] Xuemei Fan,[1] and Yingjie Xu[1,6]

[1]Department of Biochemistry and Molecular Cell Biology, Shanghai Key Laboratory for Tumor Microenvironment and Inflammation, Shanghai Jiao Tong University School of Medicine, Shanghai 200025, P.R. China; [2]State Key Laboratory of Medical Genomics, Shanghai Institute of Hematology, Collaborative Innovation Center of Hematology, Ruijin Hospital Affiliated to Shanghai Jiao Tong University School of Medicine, Shanghai 200025, P.R. China; [3]Shanghai RNACure Biopharma Co., Ltd., Shanghai 200438, P.R. China; [4]State Key Laboratory of Microbial Technology, Marine Biotechnology Research Center, Shandong University, Qingdao 266237, P.R. China; [5]State Key Laboratory of Genetic Engineering, School of Life Sciences, Zhongshan Hospital, Fudan University, Shanghai 200438, P.R. China; [6]Key Laboratory of Cell Differentiation and Apoptosis of Chinese Ministry of Education; Shanghai Jiao Tong University School of Medicine, Shanghai 200025, P.R. China

The use of messenger RNA (mRNA) enables the transient production of therapeutic proteins with stable and predictable translational kinetics and without the risk of insertional mutagenesis. Recent findings highlight the enormous potential of mRNA-based therapeutics. Here, we describe the synthesis of chemically modified thrombopoietin (TPO) mRNA through *in vitro* transcription and *in vivo* delivery via lipid nanoparticles (LNPs). After delivery of TPO mRNA in mice, compared with normal physiological values, plasma TPO protein levels increased over 1000-fold in a dose-dependent manner. Moreover, through a single intravenous dose of TPO mRNA-loaded LNPs, both reticulated and total platelet count increased significantly in mice, demonstrating that TPO protein derived from the exogenous mRNA was able to maintain normal activity. Submicrogram quantity of N_1-methylpseudouridine-modified TPO mRNA showed a similar effect in promoting thrombopoiesis as that by the TPO receptor agonist romiplostim. In addition, a therapeutic value was established in anti-GPIbα (CD42b) antibody-induced thrombocytopenia mouse models that showed a fast recovery of platelet count. Our study demonstrated chemically modified *in-vitro*-transcribed TPO mRNA as a potentially safe therapeutic intervention to stimulate thrombopoiesis.

INTRODUCTION

Thrombopoietin (TPO) is a critical physical regulator of megakaryopoiesis.[1] TPO receptor c-Mpl binding activates the Janus kinase-signal transducer and activator of transcription (JAK-STAT) pathway, thus stimulating megakaryocyte growth and platelet production.[2] TPO is produced at a constant rate mainly by the liver and then circulates in plasma, where it is sequestered by platelets and megakaryocytes via binding to c-Mpl.[3] Clinically, this feedback loop results in an inverse relationship between plasma TPO concentration and circulating platelet count.[4] Given the critical role of TPO in stimulating thrombopoiesis, TPO supplementation may be a simple and effective way to treat thrombocytopenia. Thus far, no medication has been shown to significantly increase natural hepatic TPO production. Early recombinant TPO increased platelet count in patients with immune and chemotherapy-induced thrombocytopenia[5,6]; however, it also led to the development of neutralizing anti-TPO antibodies that produce a paradoxical thrombocytopenia effect and ended their clinical development.[7] Since the initial clinical observation with the recombinant TPO protein was promising, TPO receptor agonists (TPO-RA), such as romiplostim and eltrombopag, have been developed.[8,9] Both molecules activate c-Mpl through different mechanisms, leading to an increase in megakaryocyte progenitor proliferation and platelet production.[10,11] Although both TPO mimetics have been effective in treating immune thrombocytopenia (ITP) and hepatitis C-related thrombocytopenia with good safety and tolerability, they have been associated with an increased risk of thrombocytosis and disease recurrence after stopping the drug.[12] We aimed to develop a safer and more physiological approach for boosting platelet production and treating thrombocytopenia.

Recently, the remarkable effectiveness of mRNA vaccines against COVID-19 highlights the potential of mRNA-based therapeutics as a novel drug class in the fight against many diseases.[13] *In-vitro*-transcribed (IVT) mRNA structurally resembles naturally occurring mature and processed eukaryotic mRNA and allows the translational

Received 19 January 2022; accepted 10 August 2022;
https://doi.org/10.1016/j.omtn.2022.08.017.

Correspondence: Yingjie Xu, Department of Biochemistry and Molecular Cell Biology, Shanghai Key Laboratory for Tumor Microenvironment and Inflammation, Shanghai Jiao Tong University School of Medicine, Shanghai 200025, P.R. China.
E-mail: xuyingjie@shsmu.edu.cn
Correspondence: Xuemei Fan, Department of Biochemistry and Molecular Cell Biology, Shanghai Key Laboratory for Tumor Microenvironment and Inflammation, Shanghai Jiao Tong University School of Medicine, Shanghai 200025, P.R. China.
E-mail: fanxuemei@sjtu.edu.cn

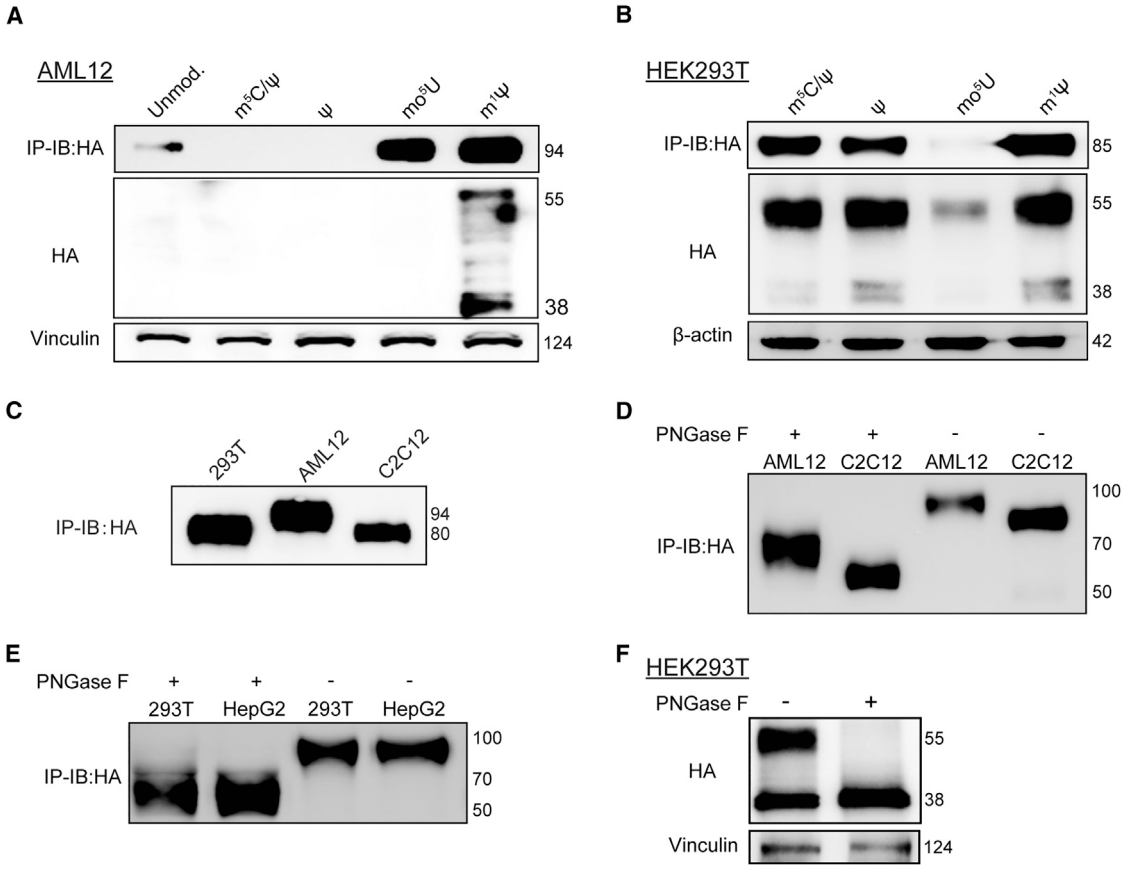

Figure 1. Sequence-engineered TPO mRNA yielded high TPO expression *in vitro*

(A) Expression of HA-tagged mouse TPO mRNA with different nucleotide modifications in AML12 cells. Unmod, uridine without any modification; m^5C/Ψ, 5-methylcytosine and pseudouridine; Ψ, pseudouridine; mo^5U, 5-methoxyuridine; $m^1\Psi$, N_1-methylpseudouridine. IP-IB: HA, HA-tagged proteins in cell culture supernatant were immunoprecipitated using anti-HA magnetic beads followed by western blot with anti-HA antibody. (B) Expression of HA-tagged human TPO mRNA with different nucleotide modifications in HEK293T cells. (C) Molecular weight of mouse TPO secreted by different types of cells. (D) Molecular weight of N-glycans removed from mouse TPO secreted by AML12 and C2C12 cells. PNGase treatment could remove N-glycans on protein. (E) Molecular weight of N-glycans removed from human TPO secreted by HEK293T and HepG2 cells. (F) Molecular weight of human TPO-HA after removal of N-glycans by PNGase F treatment in the whole cell lysates of HEK293T.

machinery of the host cells to produce many copies of the encoded protein, which can replace or supplement endogenous proteins or act as antigens to stimulate an immune response.[14] Over the past decade, major technological innovations have enabled mRNAs to become promising therapeutic tools in the field of infectious disease vaccine,[15–17] tumor immunotherapy,[18–20] protein replacement therapy,[21–23] and genome engineering.[24,25] First, various chemical modifications downregulate the immunogenicity of the mRNA and improve its stability and translational efficacy.[26–29] Second, an efficient *in vivo* delivery platform packages the mRNA to allow sufficient uptake and expression in the cytoplasm.[30] In addition to its advantage of not entering the nucleus, IVT mRNA is relatively transiently active and can be degraded physiologically. Therefore, IVT mRNA has a broad range of potential pharmaceutical applications.

In this study, we demonstrated that platelet production can be induced by chemically modified IVT-TPO mRNA, providing a proof-of-concept that mRNA-based therapeutics are a promising and novel approach for thrombocytopenia treatment.

RESULTS

Expression of TPO mRNA *in vitro*

Owing to concerns regarding poor expression levels and strong immunogenicity of IVT mRNA without chemical modification, we evaluated five mRNA molecules with various modified nucleotides using a codon-optimized TPO template tagged with HA. AML12 was used to evaluate TPO mRNA expression levels in the liver under physiological conditions. 12 h after transfection of TPO mRNA, we detected a precursor protein with a molecular weight (MW) of 38 kDa, an additional 55 kDa band in the whole cell lysate, and a 94 kDa glycoprotein in the supernatant (Figure 1A). The glycoprotein is released into the supernatant without apparent intracellular storage. This result indicates that IVT mRNA instructs cells to produce proteins that are properly assembled and have a natural glycosylation

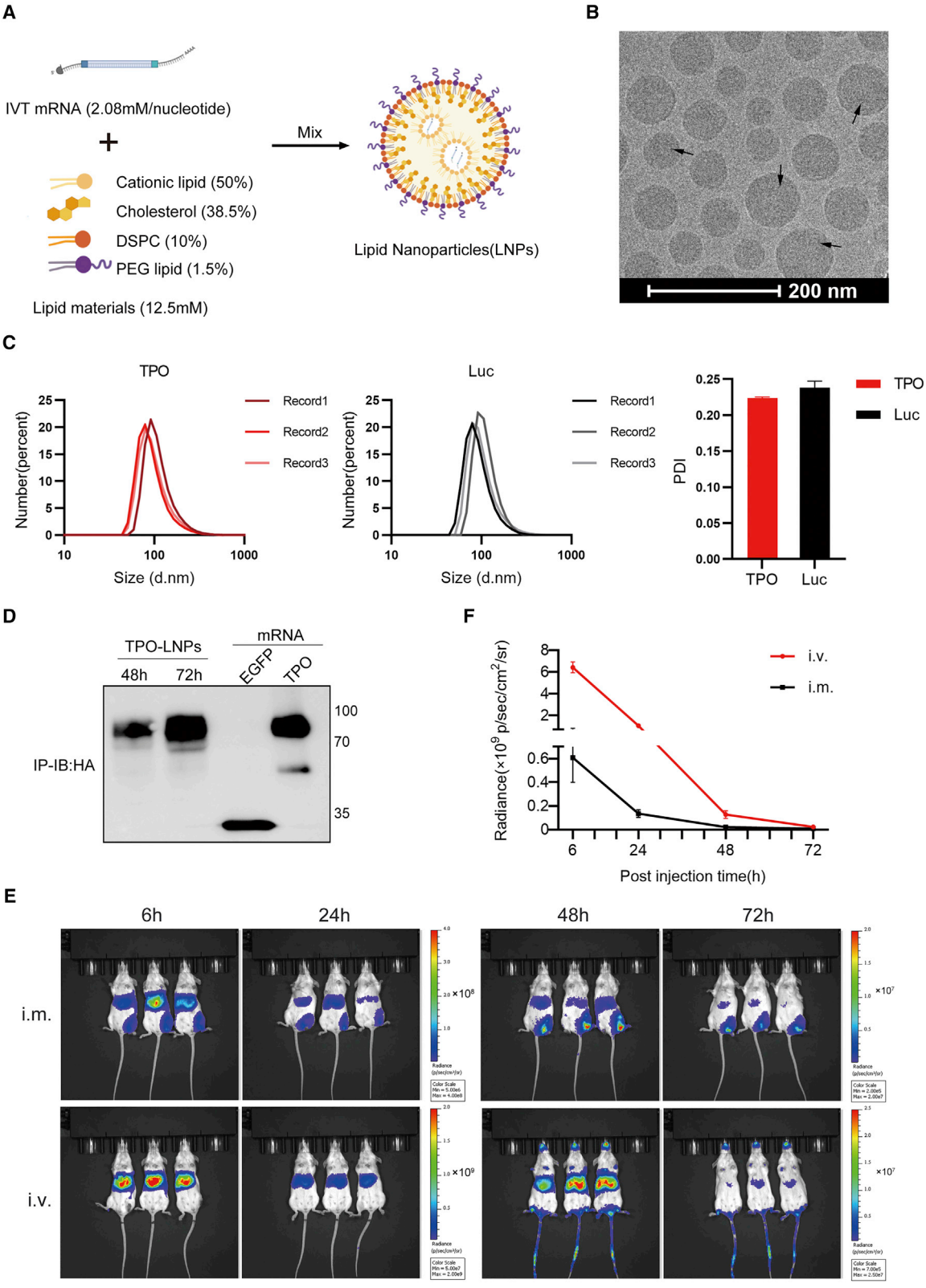

(legend on next page)

pattern. Notably, incorporation of N_1-methylpseudo-UTP ($m^1\Psi$) improved the expression of TPO in both mice and human cells (Figures 1A and 1B). Consistent with previous findings, N_1-methylpseudo-UTP-modified mRNA elicited a lower immune response compared with unmodified mRNA in both human and mouse cells, as measured by quantitative PCR of immune response marker genes (Figure S1). Interestingly, we observed a difference in the MW of TPO secreted by mouse liver cells (AML12) and myoblast cells (C2C12) (Figure 1C). Since glycosylation is the most abundant post-translational modification (PTM) of TPO, we suppose that the difference in MW may have resulted from discrepant glycosylation. After deglycosylation by PNGase F, most N-glycans were released, as indicated by the downward shift from 94 to 65 kDa and 80 to 50 kDa for TPO expressed in AML12 and C2C12, respectively (Figure 1D). This suggests that PTMs other than N-glycosylation exist in different mouse cell types. However, no difference was observed between human hepatic cells and other human cells (Figure 1E). Interestingly, digestion with PNGase F resulted in conversion of the 55 kDa band to 38 kDa band in the whole-cell lysate (Figure 1F). Since the MW shift was close to the predicted cleavage size of the N-glycan moiety, this result suggested that the 55 kDa band in the whole-cell lysate was TPO with N-glycosylation.

Expression and biodistribution of lipid nanoparticle-packaged mRNA

Since mRNA is unstable in the circulatory system and easily degraded by RNase, we employed lipid nanoparticle (LNP) encapsulation as a strategy to elicit efficient mRNA transfection *in vivo* (Figure 2A).[30] Cryo-transmission electron microscopy (cryo-TEM) image showed the size of the LNPs and effective encapsulation of TPO mRNA (Figure 2B). The mRNA-LNPs were approximately 100 nm in diameter and had a polydispersity index (PDI) of 0.2–0.25 (Figure 2C), measured using Malvern Zetasizer Nano ZS. TPO mRNA-LNP mediated a highly efficient transfection of HEK293T cells, which resulted in abundant TPO secretion (Figure 2D). To examine the duration and biodistribution of protein production by mRNA-LNPs *in vivo*, 0.5 mg/kg luciferase mRNA-LNPs were administered into mice by intravenous (i.v.) and intramuscular (i.m.) injections. The i.v. administration resulted in mRNA-LNPs being delivered to the liver, while the i.m. route targeted both the liver and the injection site (Figure 2E). In the liver, luciferase mRNA was translated, and a strong bioluminescence signal was recorded in the first 24 h after injection. Translation rate decreased quickly in the liver, showing an approximately 10-fold decrease per day. Quantification of luminescence values indicated that i.v. delivery is far more efficient than i.m. delivery. However, protein expression in the muscle decayed slowly and tended to last longer (Figures 2E and 2F).

Physiological response of mice injected with TPO mRNA-LNPs

To determine whether TPO mRNA administered *in vivo* can elevate plasma TPO levels, TPO mRNA-LNPs were injected into adult mice. 6 h after i.v. LNP delivery, plasma TPO concentration reached a maximum of more than 2000-fold in comparison to the physiological level (Figure 3A). Dose titration revealed a dose-dependent relationship between the amount of TPO mRNA administrated and the increase in plasma TPO concentration (Figures 3B and S2A). 6 h after TPO mRNA-LNP injection, we detected the expression of TPO in liver tissue by immunohistochemical analysis, which showed selective deposition in the intercellular space (Figure 3C). All i.v. LNP deliveries effectively increased circulating TPO. However, i.m. injection resulted in much lower TPO levels (10-fold after 24 h), and a dosage of less than 0.25 mg/kg mRNA-LNPs delivered by i.m. route slightly raised TPO levels in circulation (Figure 3D). Remarkably, TPO levels remained elevated for up to 7 days after i.v. administration of 0.75 mg/kg TPO mRNA-LNPs, while i.m. injection of the same amount of mRNA resulted in much lower plasma TPO concentration that declined to baseline levels by day 4 (Figure 3A).

Since TPO boosts platelet production by promoting the proliferation and differentiation of megakaryocyte precursor cells, the proportion of reticulated platelets (RPs) could be an index of thrombocytosis.[31] A significant increase in RP% was observed as early as 2 days after i.v. injection. It then reached a maximum on day 3 and returned to the pre-injection baseline (~5%) by day 6 (Figures 3E and S2B). Higher TPO mRNA levels were correlated with a higher percentage of circulating RPs. The i.v.-delivered TPO mRNA promoted thrombocytosis more potently, with a peak of nearly 40% RPs at 72 h, while i.m.-delivered mRNA also increased RP counts significantly, although not as potently as that after delivering mRNA via the i.v. route (Figure 3F).

In line with the above findings, a single dose of TPO mRNA-LNPs led to a significant elevation in the platelet count as early as 3 days post-injection, reaching a maximum on days 4–6, remaining elevated for 1 week, and then returning to baseline levels by day 10 (Figures 4A and 4B). We found no increase of platelet count at any time when luciferase-encoding mRNA-LNPs were injected, demonstrating that the effects were not due to exogenous mRNA administration but

Figure 2. Expression and biodistribution of lipid nanoparticle-packaged mRNA

(A) Scheme of LNPs packaging. Percentages in brackets show molar ratios of lipids, and concentration of mRNA represents molar concentration of nucleotides. DSPC, 1,2-distearoyl-sn-glycero-3-phosphocholine; PEG, polyethylene glycol. (B) Cryo-TEM images of TPO mRNA-LNPs. mRNA was encapsulated as arrows indicated. (C) Particle size distribution and polydispersity index (PDI) of LNPs. d.nm, diameter (nm). Error bas represent the SD (n = 3). (D) Whole cell lysates were prepared from HEK293T cells treated with TPO mRNA-LNP or transfected with HA-tagged EGFP and TPO mRNA using lipofectamine 2000. HA-tagged proteins in cell culture supernatant were immunoprecipitated using anti-HA magnetic beads, followed by western blot with anti-HA antibody. (E) *In vivo* imaging at different time points after 0.5 mg/kg luc mRNA-LNPs were administered in mice. Duration and biodistribution of mRNA-LNPs in mice administered through intravenous and intramuscular injection were recorded. Different scale of luminescence is indicated for different groups. (F) Bioluminescence intensity quantification after luciferase (luc) mRNA-LNPs were delivered through intravenous and intramuscular injection. Error bars represent the SEM (n = 3).

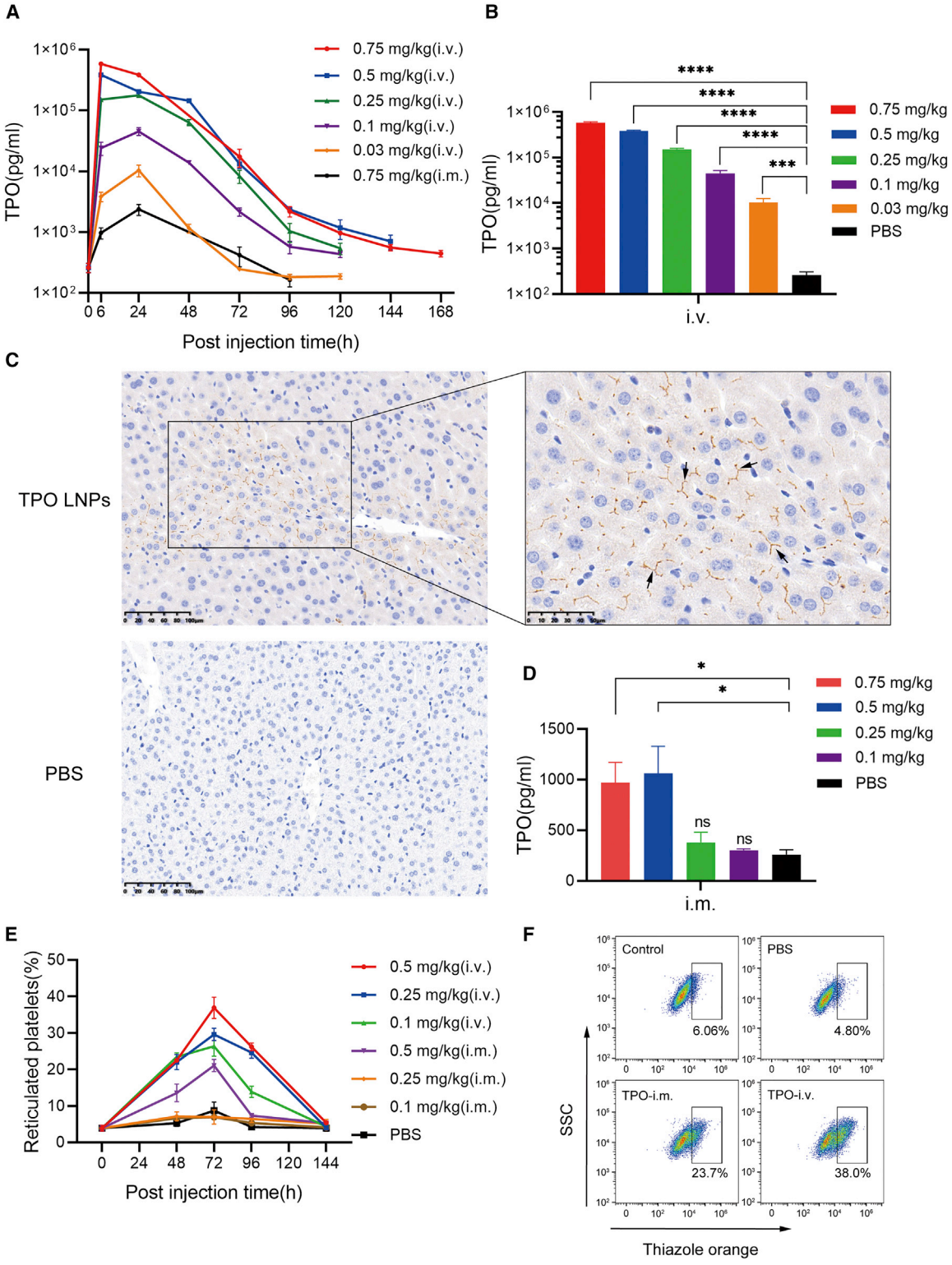

Figure 3. TPO mRNA-LNPs generated TPO *in vivo* and stimulated thrombocytopoiesis effectively

(A) TPO concentrations in mouse plasma at different post-injection times were measured with ELISA. Error bars represent the SEM (n = 4). (B) Comparison of the highest TPO concentrations after intravenous delivery of different dosages of TPO mRNA-LNPs. Error bars represent the SEM (n = 4). ***p < 0.001 and ****p < 0.0001.

(legend continued on next page)

due to functional TPO produced from the IVT-TPO mRNA. Administration of TPO mRNA-LNPs resulted in elevated TPO levels, RP%, and platelet counts in a dose-dependent manner from the 0.1 to 0.5 mg/kg dosage range in all groups. Interestingly, lower doses of TPO mRNA-LNPs increased the platelet counts earlier. Moreover, given the fact that delivery by the i.v. route raised TPO concentration 200 times more than that by the i.m. route, while there was only a 2-fold difference in platelet count (5.77 versus 3.20 times increase at the dosage of 0.5 mg/kg) (Figures 4A and 4B), the dosage of i.v.-delivered mRNA may be further reduced.

To compare the effect of TPO mRNA with thrombopoietin receptor agonist romiplostim and recombinant TPO protein in terms of stimulating platelet production, we injected the same dose of the above molecules and measured the platelet count. We found that TPO mRNA-LNPs showed a similar effect to romiplostim in terms of lag time, maximum response, and duration of efficacy (Figure 4C). Moreover, a remarkable effect was observed in low-dose (submicrogram) TPO mRNA-LNPs and romiplostim treatment (Figure 4D). By contrast, a high dosage of recombinant TPO protein only slightly increased platelet level (Figure 4C), which may be owing to its short half-life *in vivo*.

As the effect of TPO mRNA in thrombocytosis promotion lasts for a week, repeated administration may be used as a clinical strategy. Therefore, we tested the effect of repeated injection of TPO mRNA-LNPs on thrombocytosis promotion 1 week after the platelet count returned to baseline after the first injection. Interestingly, a second dose of TPO mRNA-LNPs (0.1 mg/kg) elevated platelet count as early as 48 h post-administration and maintained the elevated level for a week (Figure 4E). We assumed that this may result from more megakaryocyte precursor cells being produced by the first TPO mRNA injection. Consistent with this finding, weekly injections of TPO mRNA-LNPs or romiplostim efficiently increased the platelet count for 4 weeks (Figure 4F).

Therapeutic efficacy of TPO mRNA-LNPs in thrombocytopenia mouse models

ITP is a disease characterized by abnormally low levels of platelet, mainly caused by an immune system attack.[32] To establish a thrombocytopenia mouse model, we used R300, a mixture of purified rat monoclonal antibodies that specifically reacts with mouse GPIbα (CD42b). Targeting GPIbα with R300 leads to irreversible platelet depletion in mice by Fc-independent mechanism. Here, we established two ITP models using R300 delivered via different routes, i.v. and subcutaneous delivery, which resulted in rapid and chronic platelet clearance, respectively.[33] A dosage of 0.25 mg/kg i.v. R300 could deplete >90% platelets within 1 h, followed by recovery of platelets 3 days later (Figure 5A). There was a temporary elevation of plasma TPO concentration when platelets were cleared upon R300 treatment (Figure 5B). Given the lag time of TPO mRNA to increase platelet production, we injected TPO mRNA-LNPs 1 day/2 days before R300 administration. The dose of 0.1 mg/kg i.v.-delivered TPO mRNA-LNPs showed a protective effect for rapid recovery of platelets and maintaining platelet count higher than baseline levels, and the effect lasted for 4–5 days (Figure 5C). By contrast, subcutaneous injection of low-dose R300 (0.08 mg/kg) every 3 days lowered the platelet level gradually (Figure 5D). When the platelet count was reduced to approximately 10% of the basal amount, upregulation of TPO levels was also observed (Figure 5E). In the prolonged thrombocytopenia model, we evaluated the therapeutic effect of TPO mRNA-LNPs, romiplostim, and recombinant TPO protein. We found that both TPO mRNA-LNPs and romiplostim effectively elevated platelet counts to a level higher than baseline levels at day 5 after injection of the first R300 dose and remained elevated for 5–6 days (Figure 5F). However, when the same dosage (0.1 mg/kg) of recombinant TPO was administered, there was barely any effect (Figure 5F). Both recombinant TPO and romiplostim had no effect on plasma TPO levels (Figure S3), which may be explained by the short half-life of recombinant TPO without modification. Notably, submicrogram amounts of TPO mRNA-LNPs and romiplostim injection showed remarkable therapeutic efficacy, as demonstrated by the fast recovery of the platelet levels (Figure 5G).

In vivo safety profile of TPO mRNA-LNPs

To evaluate the *in vivo* side effects of mRNA-LNPs, various organs were collected 1 day after the last bleeding (day 26) in the repeated injection experiment (Figure 4E). No histological differences were found in the tissues from the heart, liver, spleen, or kidney between phosphate-buffered saline (PBS) and TPO mRNA-LNP treatment groups, suggesting no notable toxicity (Figure 6A). Since i.v.-injected TPO mRNA-LNPs were mainly distributed and expressed in the liver, we checked the concentrations of aspartate aminotransferase (AST) and alanine aminotransferase (ALT) to assess liver function and found no obvious changes in these parameters in the serum collected from TPO mRNA-LNP-injected mice (Figures 6B and 6C). Since bone marrow fibrosis has been reported in animals and patients receiving TPO-RAs,[34] we investigated whether TPO mRNA-LNPs result in reticulin deposition. In mice with four repeated weekly doses of TPO mRNA-LNPs or romiplostim, hematoxylin and eosin (H&E) and reticulin stains of bone marrow tissue sections from femurs showed an absence of reticulin fibrosis (Figure 6D).

We also investigated the immune response to TPO mRNA-LNPs by measuring the concentration of the proinflammatory cytokine tumor necrosis factor alpha (TNF-α). The level of TNF-α (minimum

(C) Immunohistochemistry shows expression of HA-tagged TPO (black arrows) in mouse liver tissue 6 h after administration of 0.1 mg/kg TPO mRNA-LNPs. The right panel shows an image of the inset box in a higher magnification. (D) Comparison of TPO concentrations 6 h after intramuscular delivery of different dosages of TPO mRNA-LNPs. Error bars represent the SEM (n = 4). *p < 0.05. (E) Percentage of RPs as measured by flow cytometry using thiazole orange staining. TPO mRNA-LNPs were delivered through different routes and in different dosages. The change of RP% in all groups over time is indicated. Error bars represent the SEM (n = 4). (F) Dot plots showing the distribution of thiazole-positive events in platelets in the whole blood as 0.5 mg/kg TPO mRNA-LNPs were delivered through different routes. SSC, side scatter.

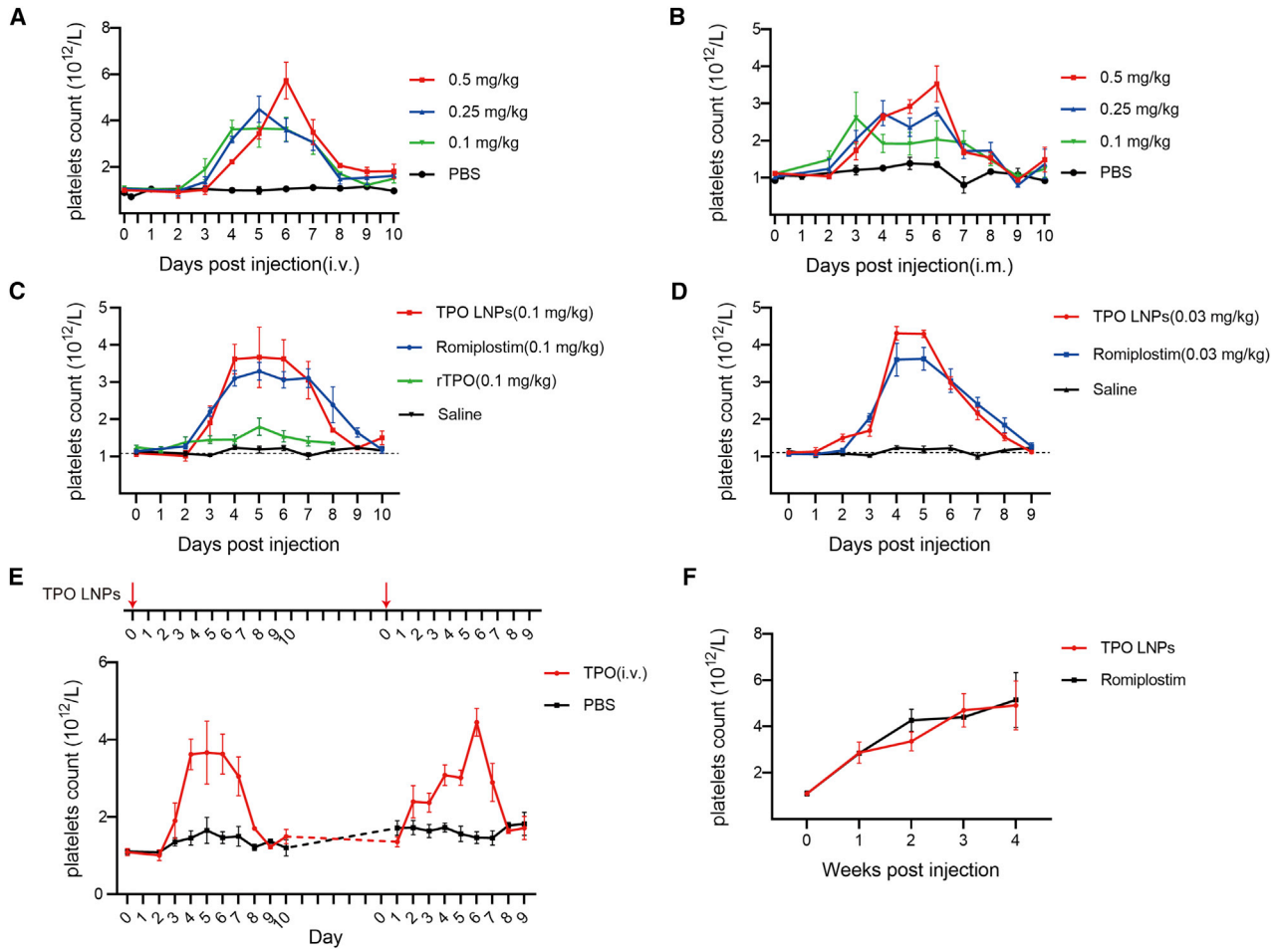

Figure 4. TPO mRNA-LNPs elevated platelet count in mice

(A) Mouse platelets were counted after intravenous and (B) intramuscular TPO mRNA-LNP injections. Error bars represent the SEM (n = 4). (C) The therapeutic effects of TPO mRNA-LNPs, romiplostim, and recombinant TPO protein were compared at dosages of 0.1 mg/kg and (D) 0.03 mg/kg. TPO mRNA-LNPs were delivered through tail vein. Romiplostim was injected subcutaneously, and recombinant TPO was injected intraperitoneally. Error bars represent the SEM (n = 5). (E) Platelet count was recorded as intravenous injection of 0.1 mg/kg TPO mRNA-LNPs was repeated twice. Second injection was conducted 1 week after the platelet count returned to baseline upon the first injection. Error bars represent the SEM (n = 4). Red arrows indicate the time points at which the TPO mRNA-LNP injections were administered. (F) Platelet count was recorded as four administrations of TPO mRNA-LNPs and romiplostim (both 0.1 mg/kg) were repeated weekly. Error bars represent the SEM.

level: 30.8 pg/mL) was not detected in the serum of mice 6 h and 24 h after the injection of TPO mRNA-LNPs, indicating no significant cytokine response (Figure S4A).

Repeated dosing also raises the concern of inducing anti-TPO-antibodies. We checked for the presence of anti-TPO-antibodies using ELISA, and no anti-TPO antibodies were detected after four repeated injections of TPO mRNA-LNPs (Figure S4B). TPO mRNA-LNPs had no significant impact on red blood cells but induced a temporary decline in white blood cells that was recovered within 2 days (Figures S4C and S4D). Moreover, we found no obvious changes in liver morphology and functional parameters in serum, including AST and ALT levels, after repeated TPO mRNA-LNPs injections (Figure S5), further indicating negligible side effects.

DISCUSSION

In this study, we demonstrated that a single submicrogram dose of chemically modified TPO mRNA is sufficient to elevate plasma TPO levels as early as 6 h after injection. Importantly, TPO mRNA increases the platelet count as fast as that by TPO-RA romiplostim in both normal and thrombocytopenia mouse models. After 4 weeks of once-weekly administration, the responses to TPO mRNA-LNPs were generally sustained as long as treatment continued regularly. In addition to efficacy, TPO mRNA-LNPs showed no significant adverse side effects or detectable cytokine responses. These remarkable therapeutic properties were achieved through a combination of codon optimization, the incorporation of chemically modified nucleotides into mRNA, and an efficient delivery platform.

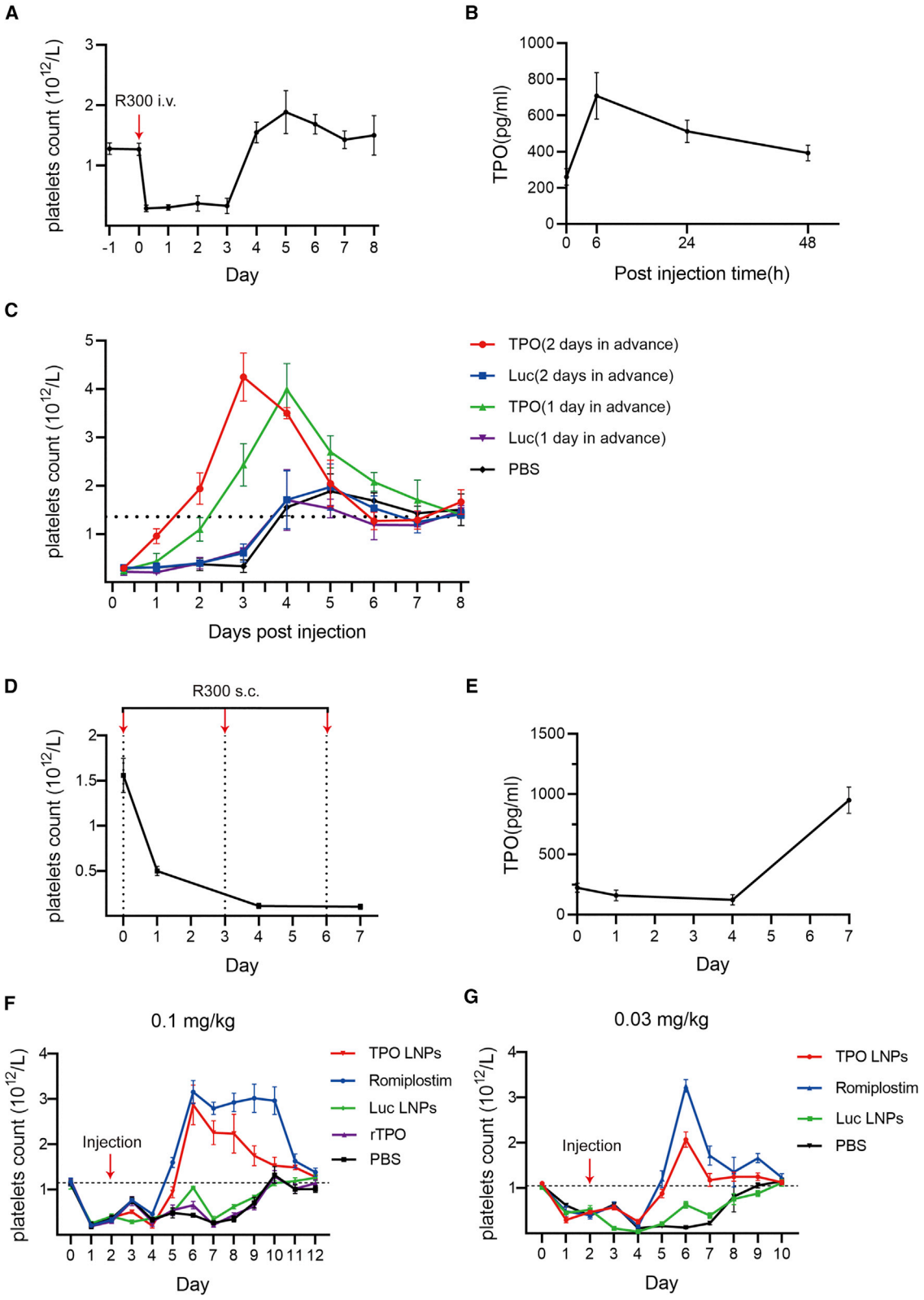

(legend on next page)

Before the approval of TPO-RA, treatment options for thrombocytopenia mainly consisted of platelet transfusion, corticosteroids, immunoglobulins, or splenectomy.[35] While these strategies often effectively elevated the platelet count, the costs and risks were substantial. Since TPO affects nearly all stages of thrombopoiesis to stimulate the proliferation and maturation of megakaryocytes and subsequent platelet production, TPO and its receptor have been the main focus for the development of pharmacological treatment for thrombocytopenia.[36] The development of recombinant human TPO (rhTPO) and pegylated rhTPO (PEG-rhTPO) has been halted because anti-TPO antibodies have been shown to develop in healthy individuals; these can cross-react with endogenous TPO to induce thrombocytopenia.[7] Second-generation TPO-RAs romiplostim and eltrombopag have been demonstrated to be highly effective[10,37]; however, there are several major concerns regarding the use of TPO-RAs in patients with ITP, including the risk of bone marrow fibrosis, rebound thrombocytopenia when TPO-RA is abruptly stopped, and increased thrombosis in patients with underlying hypercoagulable statuses.[38] For patients with ITP who fail TPO-RA or are unable to receive it, there are several alternative therapeutic options, including rituximab, fostamatinib, mycophenolate mofetil, dapsone, and danazol.[36] New therapeutic strategies are necessary to treat patients with more complicated and refractory thrombocytopenia. By subjecting itself to the host cell's translational machinery, IVT mRNA has groundbreaking potential as a new class of drugs for protein supplementation therapy.

It is well known that the strategy of mRNA-based therapeutics was enabled by the preceding achievements of mRNA modification to avoid undesired immune reaction and increased protein expression.[26] Consistently, we found that N_1-methylpseudouridine-modified mRNAs elicited a lower response for most immune response markers compared with unmodified mRNA in both human and mouse cell lines. Moreover, in different cell lines, IVT mRNA with different chemical modification resulted in different protein expression level. This finding suggested that the translation efficiency of IVT mRNA may be determined by translational machinery of the cells in a nucleotide modification-dependent manner. Further studies are needed to unravel the underlying mechanisms of this cell dependency. Based on this finding, it will be necessary to screen the expression of IVT mRNA with chemical modifications on target cells before performing *in vivo* experiments.

IVT-TPO mRNA has two major advantages over recombinant TPO and TPO-RAs. First, i.v.-delivered IVT-TPO mRNA can efficiently increase production of hepatic TPO, harboring natural PTMs that dramatically enhance the capability of TPO. The sustained expression of proteins by host cells offsets the short protein half-life compared with that of recombinant TPO. In addition, given the predicable *in vivo* protein translational kinetics of IVT mRNA, TPO concentration is tunable as a good dose-effect relationship and similar pharmacokinetics for all doses were observed. Second, TPO mRNA-LNPs showed therapeutic efficacy similar to that of TPO-RA romiplostim without any detectable adverse side effects. Since the translated TPO from IVT-TPO mRNA is also subject to physiological regulation by the negative feedback loop,[39] the amount of TPO is regulated by platelet c-Mpl receptor-mediated uptake and destruction, preventing sustained stimulation of megakaryopoiesis. As concerns have been raised regarding the risk of developing bone marrow fibrosis by TPO-RA, further investigation of the long-term safety profiles of TPO mRNA-LNP in animal models is needed, including assessment of possible induction of bone marrow fibrosis as well as continuous stimulation of the hematopoietic stem cell compartment.

mRNA-LNPs have been reported in protein replacement/supplemental therapy in mouse models of diseases caused by lack of protein or defective protein.[40–43] To achieve sustained expression of functional proteins, these clinical applications require repeated administration. In this study, we introduced a single submicrogram dose of chemically modified TPO mRNA to boost robust TPO expression and consequently promote platelet production. However, the tissue-specific delivery of mRNA through systemic administration remains a challenge. When injected by i.v. route, mRNA-LNPs mainly target the liver by absorption of serum apolipoprotein E, which in turn binds low-density lipoprotein receptors on the surface of hepatocytes.[44] Since TPO is produced predominantly by hepatocytes, the current LNP delivery system is feasible for application. Notably, the relatively long *in vivo* survival of TPO produced via the i.v. route may be explained both by more efficient TPO secretion and the more physiological PTMs of TPO produced by liver cells when compared with those produced by muscle cells. In addition, our results showed that a very low dosage of TPO mRNA-LNPs could induce effective platelet count promotion, similar to a high dosage of TPO mRNA-LNPs. No thrombocythemia was observed in our study, even in the group with highest TPO mRNA-LNPs dose. We hypothesized that maintaining a relatively high TPO concentration could be a better strategy than inducing a high pulse in the treatment of chronic ITP. It has been reported that sustained release of nanoparticles and subsequently prolonged expression of target proteins can be achieved by introducing poly (D,

Figure 5. Therapeutic efficacy of TPO mRNA-LNPs in mouse thrombocytopenia models

(A) Platelet count of acute thrombocytopenia model generated by intravenous injection of 0.25 mg/kg R300. Error bars represent the SEM (n = 4). (B) TPO levels increased on the first day after injection in the acute thrombocytopenia model. Error bars represent the SEM (n = 4). (C) TPO mRNA-LNPs promoted thrombopoiesis in the acute thrombocytopenia model. R300 was injected to deplete platelets at day 0, and LNPs were injected 1–2 days in advance. Error bars represent the SEM (n = 4). (D) Platelet count of prolonged thrombocytopenia model generated by repeated subcutaneous injection of low-dose R300. Each single dose was 0.08 mg/kg, and red arrows indicate the date of injection. Error bars represent the SEM (n = 5). (E) TPO levels in the prolonged thrombocytopenia model were measured with ELISA. Error bars represent the SD (n = 4). In the prolonged thrombocytopenia model, the therapeutic effects of TPO mRNA-LNPs, romiplostim, and recombinant TPO protein were compared at the dosages of 0.1 mg/kg (F) and 0.03 mg/kg (G). Red arrows indicate the date of injection. TPO mRNA-LNPs were injected through tail vein. Romiplostim was injected subcutaneously, and recombinant TPO was injected intraperitoneally. Dose and injection date of R300 was the same in (D). Error bars represent the SEM (n = 5).

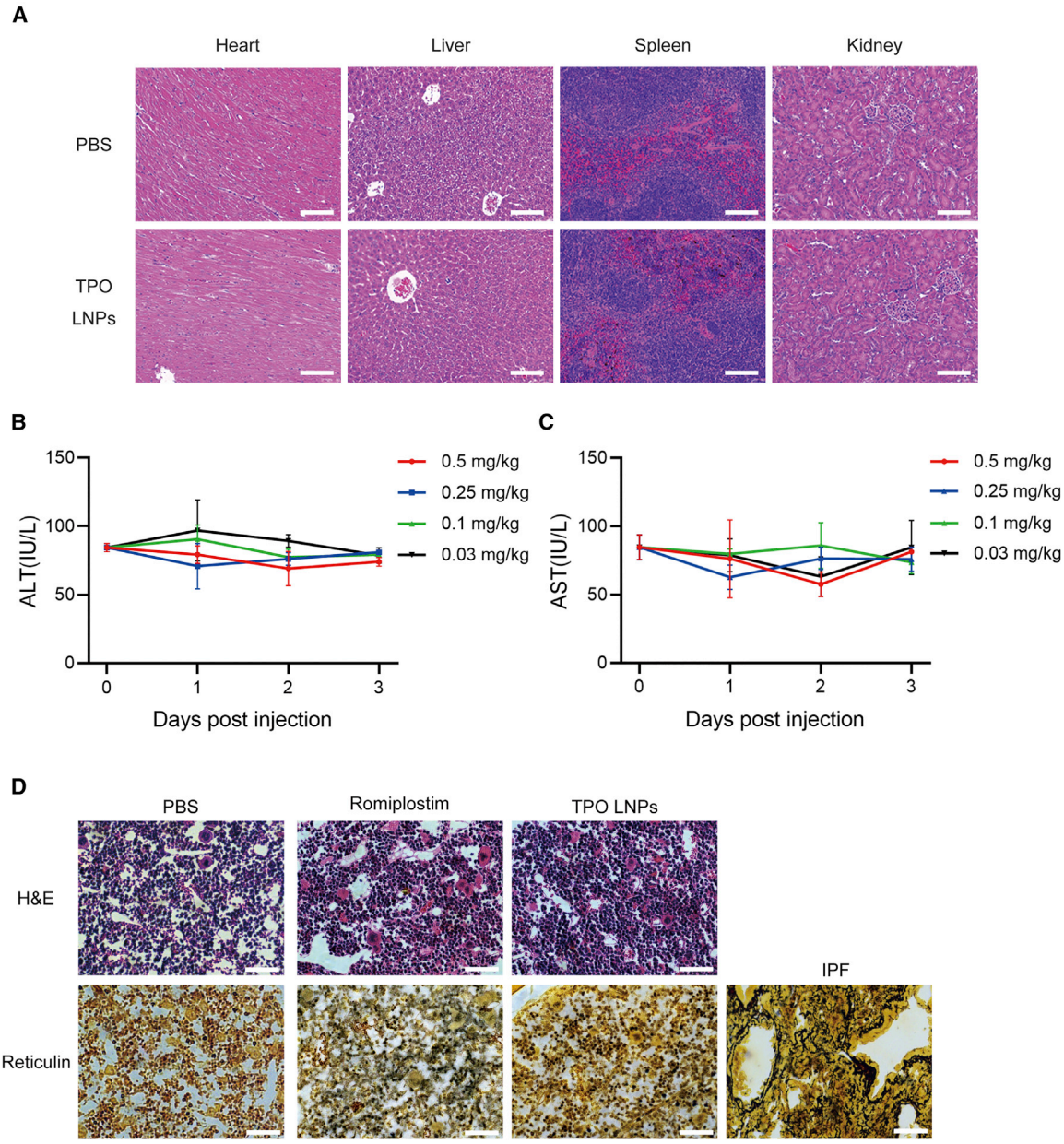

Figure 6. *In vivo* safety profile of TPO mRNA-LNPs

(A) Hematoxylin and eosin (H&E) staining of heart, liver, spleen, or kidney sections from the PBS and TPO mRNA-LNP treatment groups in the repeated injection experiment in Figure 4E. Scale bar, 100 μm. No obvious changes were found in (B) ALT and (C) AST levels after different doses of TPO mRNA-LNPs administration. Error bars represent the SD (n = 3). (D) H&E and reticulin staining of bone marrow after four weekly repeated injections of romiplostim and TPO mRNA-LNPs. Scale bar, 50 μm. Idiopathic pulmonary fibrosis (IPF) model sections were shown to be a positive control of reticulin staining.

L-lactic-co-glycolic acid) (PLGA) in nanoparticle formulation, which may be a direction for further improvement.[45,46]

We found that TPO mRNA-LNPs (both 0.1 mg/kg and 0.03 mg/kg) showed similar effects to romiplostim in normal mice in terms of lag time, maximum response, and duration of efficacy. However, in the antibody-induced prolonged thrombocytopenia model, romiplostim injection showed higher and longer lasting platelet counts compared with TPO mRNA-LNPs. It has been reported that antibody-induced platelet apoptosis resulted in clearance of platelets via hepatocyte capture and Kupffer cell phagocytosis.[33,47,48] We think that above process may have impact on the amount of TPO mRNA-LNP in the circulation or interfere with the uptake of TPO mRNA-LNP by hepatocytes and the subsequent production of TPO protein, which explains the

lower and shorter duration of platelet count in the TPO mRNA-LNPs treatment group compared with the romiplostim treatment group. To better compare the therapeutic efficacy of TPO mRNA-LNPs and romiplostim, ITP models other than antibody-induced passive ITP can be employed, such as active the ITP model based on the transfer of splenocytes from mice immune against platelet CD61 into mice with severe combined immunodeficiency.[49]

Altogether, our study shows that chemically modified mRNA offers a new and promising approach for the therapeutic expression of the extracellular protein TPO. The use of chemically modified mRNA combined with an LNP delivery system enables the rapid expression of desired proteins with predictable expression kinetics, high transfection efficiency, and most importantly, without risk of chromosomal integration. Although mRNA medicines that replace or supplement beneficial proteins for the treatment of chronic diseases encounter a tougher road to the clinic than mRNA vaccines, significant advances in basic mRNA biology and optimization of large-scale mRNA synthesis and delivery platforms guarantee that the future of mRNA-based therapeutics is bright.

MATERIALS AND METHODS

Cell culture and reagents

Mouse hepatic cell line (AML12), mouse myoblast cell line (C2C12), human hepatic cancer cell line (HepG2), and human embryonic kidney cell line (HEK293T) were used in *in vitro* studies to evaluate the expression of chemically modified mRNA. All cells were purchased from the American Type Culture Collection. AML12 cells were maintained in Dulbecco's modified Eagle's medium/F12 (DMEM/F-12, L310KJ; Basalmedia, Shanghai, China) supplemented with 0.45% insulin-transferrin-selenium (ITS, S450J7; Basalmedia, Shanghai, China), while other cells were maintained in high-glucose DMEM (HyClone, Logan, UT, USA). All media were supplemented with 10% fetal bovine serum (FBS, 10099141; Gibco, Australia) and 1% penicillin–streptomycin (S110JV; Basalmedia, Shanghai, China). The cells were grown in a humidified incubator at 37°C with 5% CO_2.

Preparation of modified TPO mRNA

TPO mRNAs were synthesized *in vitro* using T7 polymerase-mediated RNA transcription as previously described.[46,50] Codon-optimized open reading frames flanking 5′ and 3′ untranslated regions (UTRs) were synthesized by General Biology (Anhui, China) and cloned into a vector downstream of a T7 promoter. The DNA templates were amplified by PCR, purified, and used for IVT. Cap1 analog (EzCap AG, B8176; APExBIO, TX, USA) was included in the IVT reaction to place a Cap1 structure at the 5′ end of mRNAs. mRNAs were synthesized using nucleotides that were either completely unmodified; had cytidine (C) fully substituted with 5-methyl-cytidine (m^5C); or uridine (U) fully substituted with modified uridine analogs, i.e., pseudouridine (Ψ), N1-methyl-pseudouridine ($m^1\Psi$), 5-methyoxy-uridine (mo^5 U), or a combination of Ψ and m^5C. Following transcription, poly(A)-tail was added to the RNA transcripts using a poly(A)-tailing kit (K1053; APExBIO, TX, USA). mRNA was purified using a MEGAclear kit (AM1908; Thermo Fischer Scientific, MA, USA), treated with Antarctic Phosphatase (M0289; New England BioLabs, MA, USA) at 37°C for 30 min and then purified.

Preparation of mRNA-loaded lipid nanoparticles

The LNP formulations were prepared as previously described.[50] Briefly, lipids were dissolved in ethanol at molar ratios of 50:10:38.5:1.5 for DLin-MC3-DMA:DSPC:cholesterol:PEG2000-DMG. The lipid mixture was mixed with an equal volume of mRNA solution in 50 mM citrate buffer (pH 3.0) using a T-mixer. The formulations were immediately diluted 2-fold with 50 mM citrate buffer (pH 3.0) and dialyzed in PBS (pH 7.4) in slide-a-lyzer dialysis cassettes (66380; Thermo Fisher Scientific, MA, USA) for at least 15 h. The formulations were concentrated using Amicon Ultra Centrifugal Filters (UFC8030; Millipore, MA, USA) and passed through a 0.22-μm filter (SLGP033RB; Millipore, MA, USA). RNA encapsulation for all formulations was determined using the Quant-iT RiboGreen RNA Assay (R11490; Thermo Fischer Scientific, MA, USA). Particle sizes were analyzed using a nanoparticle tracking analysis instrument (Zetasizer Nano ZS, Malvern, UK).

Transfection of mRNA

To evaluate the expression efficiency of modified TPO mRNA, cells were seeded in a 6-well-plate to 70%–90% confluency and transfected with 1–2 μg/well TPO mRNA using lipofectamine 2000 (11668019; Thermo Fischer Scientific, MA, USA). Complexes were prepared using an mRNA (μg) to reagent (μL) ratio of 1:2 for most cell lines.

Western blot assay

Cells were collected, washed with ice-cold Dulbecco's PBS three times and lysed in mammalian cell lysis buffer (MCLB; 50 mM Tris, pH 7.5; 150 mM NaCl; 0.5% NP40), complete EDTA-free protease inhibitor (04693159001; Roche, Basel, Switzerland), and 1 mM phenylmethylsulfonyl fluoride (PMSF, 0754; Amresco, Solon, OH, USA) on ice. Protein concentrations were determined using the Quick Start Bradford assay (5000201; Bio-Rad, Hercules, CA, USA). The same amount of protein from each sample was separated by sodium dodecyl sulfate-polyacrylamide gels electrophoresis and transferred to a nitrocellulose membrane (Millipore, MA, USA). The membranes were blocked with 5% non-fat milk (Sangon Biotech, Shanghai, China) for 1 h at room temperature and incubated with primary antibodies (1:1000) diluted in primary antibody dilution buffer (Beyotime Biotechnology, Shanghai, China) overnight at 4°C. Thereafter, the membranes were washed three times with Tris-buffered saline with Tween (TBST; 20 mM Tris, pH 7.4; 137 mM NaCl; 0.05% Tween 20) and incubated with proper diluted horseradish peroxidase-conjugated secondary antibodies at room temperature. Images were detected by enhanced chemiluminescence using the ChampChemi imaging system (Sage Creation Science, Beijing, China).

The following antibodies were used: HA-Tag (C29F4) rabbit mAb #3724 (3724; Cell Signaling Technology, MA, USA); Beta Actin Monoclonal Antibody (66009-1-Ig; Proteintech Group, IL, USA); Vinculin Monoclonal antibody (66305-1-Ig; Proteintech Group, IL, USA).

Immunoprecipitation of TPO from supernatant

Cells were grown to 70%–90% confluence and transfected with TPO-HA mRNA. 24 h after transfection, supernatant from the above cells was filtered through a 0.45-μm filter and collected into a 15-mL tube, and complete EDTA-free protease inhibitor was added. HA magnetic beads (88836; Thermo Fischer Scientific, MA, USA) were washed with MCLB and incubated with the supernatant at 4°C overnight with gentle rotation. The next day, the precipitated immunocomplexes were washed four times on a magnetic SampleRack with MCLB and boiled in 5× SDS sample buffer, followed by western blot analysis.

N-glycosylation detection

TPO secreted by cells was enriched by immunoprecipitation (IP), as described above. A 10-μL total denaturing reaction volume was made up of 10 μg TPO protein enriched by IP, 1 μL of glycoprotein denaturing buffer (10×), and H_2O (if necessary). Glycoprotein was denatured by heating at 100°C for 10 min. After chilling on ice, a total reaction volume of 20 μL was prepared by adding 2 μL GlycoBuffer 2 (10×), 2 μL of 10% NP-40, 6 μL of H_2O, and 1 μL of PNGase F (P0704S; New England Biolab, MA, USA). The reaction mix was incubated at 37°C for 2 h, followed by western blot analysis.

Cryo-TEM sample preparation and imaging

4 μL of sample was applied onto a glow-discharged grid (R2/1 Cu, 300 mesh, Quantifoil, Germany). Grids were blotted for 3 s at 100% humidity and 4°C and immersed in liquid ethane using a Mark IV vitrobot (Thermo Fisher Scientific, MA, USA). Images were acquired using a Talos F200C G2 transmission electron microscope (Thermo Fisher Scientific, MA, USA) in the low dose mode. Magnification was set to 36,000× with a pixel size of 5.75 Å.

Animals

8-week-old female normal BALB/c and C57BL/6 mice were used for biodistribution and therapeutic efficacy studies. All animal experiments were performed under strict regulations and pathogen-free conditions at the animal facility of Shanghai Jiao Tong University School of Medicine. The animal protocol was reviewed and approved by the Institutional Animal Care and Use Committees of School of Medicine, Shanghai Jiao Tong University.

Biodistribution of mRNA-LNPs *in vivo*

To study the biodistribution of LNPs in mice, six BALB/c mice were divided into two groups, and LNPs carrying luciferase mRNA (R1013; APExBIO, TX, USA) (0.5 mg/kg) were injected through the tail vein or gastrocnemius muscle. Mice were intraperitoneally injected with 150 mg/kg D-luciferin (122799; PerkinElmer, MA, USA) at 6, 24, 48, or 72 h after LNPs administration. 10 min after the injection of luciferin, the mice were imaged using IVIS Spectrum CT (128201; PerkinElmer, MA, USA). Luminescence values were quantified using the Living Image Software (PerkinElmer, MA, USA).

Measurement of plasma TPO concentration

Mouse whole-blood samples were collected from the orbital vein. An anticoagulant (White's buffer; 114 mM sodium citrate, 136 mM glucose) was added to whole blood at a proportion of 10%. Whole blood was centrifuged (2,600 × *g*, 10 min), and plasma was collected. Mouse plasma TPO levels were measured using a mouse TPO ELISA kit (ab100748; Abcam, England).

Measurement of reticulated platelets by flow cytometry

To evaluate the ability of TPO mRNA-LNPs to promote thrombopoiesis, mouse whole-blood samples were collected from the orbital vein. Anticoagulant (White's buffer) was added to whole blood at a proportion of 10% and was further diluted 10 times with Tyrode's buffer (12 mM $NaHCO_3$, 138 mM NaCl, 5.5 mM glucose, 2.9 mM KCl, 2 mM $MgCl_2$, 0.42 mM NaH_2PO_4, 10 mM HEPES). The above sample was stained with thiazole orange (390062; Sigma-Aldrich) as a platelet mRNA stain and CD41-APC (17-0411-82; Thermo Fischer Scientific, MA, USA) for platelet identification for 1 h and 30 min, respectively. The stained sample solution was diluted 10 times with Tyrode's buffer and was run on a flow cytometer (Beckman CytoFLEX S). The gate was set to maintain a normal proportion of RPs at approximately 5%. The results were analyzed using FlowJo and CytExpert software.

Platelet count

Mouse whole-blood samples were collected from the orbital vein. Anticoagulant (White's buffer) was added to whole blood at a proportion of 10% and diluted five times with saline. Platelets were counted using a Sysmex pocH-100iV Diff hematology analyzer (Sysmex, Japan).

R300-treated thrombocytopenia mouse model

A single dose of 0.25 mg/kg of the rat anti-mouse GPIbα (CD42b) monoclonal antibody R300 (R300; Emfret Analytics, Germany) was injected by i.v. route to establish an acute anti-GPIbα antibody-induced thrombocytopenia mouse model. To imitate chronic immune thrombocytopenia, we injected 0.08 mg/kg of R300 subcutaneously every 3 days to establish a prolonged thrombocytopenia mouse model. The mice were treated with TPO mRNA-LNPs, romiplostim (Amgen, CA, USA), or recombinant mouse thrombopoietin protein (ab170079; Abcam, England). TPO mRNA-LNPs were injected through the tail vein. Romiplostim was injected subcutaneously according to its instructions, while recombinant mouse thrombopoietin protein was injected intraperitoneally.

Immunohistochemistry staining of TPO-HA

For immunohistochemistry analysis, paraffin-embedded liver tissues were cut into 4-μm sections, deparaffinized in xylene, rehydrated through a graded ethanol series, and then subjected to antigen repair by citric acid using the microwave boiling method. Endogenous peroxidase activity was blocked by incubation with 3% hydrogen peroxide at room temperature for 10 min. The slides were incubated with anti-HA antibody (1:400, #3724; Cell Signaling Technology, MA, USA) overnight at 4°C in a humidified chamber. The next day, sections were washed in PBS three times for 5 min each. Secondary antibody was applied for 30 min at 37°C, and color was developed using a diaminobenzidine peroxidase substrate kit (Impact DAB, Vector

Laboratories, CA, USA). Sections were then counterstained with hematoxylin, dehydrated, and mounted.

In vivo toxicity evaluation: Histology, hematological examination of AST and ALT, immune response

For histological examination, various organs (heart, liver, spleen, and kidney) were collected 1 day after the last bleeding (day 26) in the repeated injection experiment or the second day after 4 times weekly injection. All organs were fixed overnight in 4% paraformaldehyde (E672002; Sangon Biotech, Shanghai, China) at 4°C, embedded in paraffin, sectioned, and stained with H&E according to routine protocols. For hematological examinations, whole blood was centrifuged (2,600 × *g*, 10 min), and plasma was collected. Alanine aminotransferase (ALT/GPT) and aspartate aminotransferase (AST/GOT) levels were measured following the protocols of ALT/GPT Colorimetric Assay Kit (Reitman-Frankel method) (E-BC-K235-M; Elabscience, Wuhan, China) and AST/GOT colorimetric assay kit (Reitman-Frankel method) (E-BC-K236-M; Elabscience, Wuhan, China). TNF-α levels were measured using a Mouse TNF-α ELISA Kit (PT512; Beyotime, Shanghai, China). Standards were fitted with a four-parameter logistic (4PL) curve.

Bone marrow fibrosis analysis

For bone marrow pathology, mouse femurs were separated on the fourth day after the fourth injection and fixed in 4% paraformaldehyde for 2 days at 4°C. The following steps were performed by Beyotime Biotechnology (Shanghai, China). The fixed femurs were decalcified, dehydrated, and embedded in paraffin. H&E staining and reticular fiber silver staining (Gordon and Sweet's method) were performed according to routine protocols.

Statistical analysis

All statistical analyses and graphs were prepared using the GraphPad Prism 8 software using two-sided t tests. Error bars indicate standard error of the mean (SEM) unless otherwise noted as the standard deviation (SD). Statistical significance was set at $p < 0.05$, and significant values shown in various figures are indicated as follows: $^{*}p < 0.05$, $^{**}p < 0.01$, $^{***}p < 0.001$, and $^{****}p < 0.0001$.

DATA AVAILABILITY

The main datasets supporting this study are available within the article and supplemental information. Raw data or additional data analyzed in the study are available from the corresponding authors upon reasonable request.

SUPPLEMENTAL INFORMATION

Supplemental information can be found online at https://doi.org/10.1016/j.omtn.2022.08.017.

ACKNOWLEDGMENTS

This work was in part supported by the National Natural Science Foundation of China (81970123) to X.F., Shanghai Jiao Tong University Fund for Key Foresight in Scientific and Technological Innovation (2019TPA10) to Y.X., and Shanghai Jiao Tong University School of Medicine Fund for Key innovation team-collaborative team (SHSMU-ZDCX20211801) to J. L. The authors thank Professors Han Liu, Chao Fang, Xuyun Zhao, and Lan Wang for their support. The authors thank Zheng Ruan, Qidi Chen, Mengyu Yan, Si Zhang, Maohua Zhu, Lin Zhang, Chenyue Hang, Jia Xia, Wei Zhang, and Pengcheng Yu for their assistance. The authors thank Shanghai Jiao Tong University Instrumental Center for their help with cryo-TEM. Graphical abstract and Figure 2A were created with BioRender.com.

AUTHOR CONTRIBUTIONS

Y. Z., X.F., J. L., and Y.X. conceived the idea, designed the study, and directed the project. Y.Z. performed all the experiments and analyzed data. Y.Z. and Y.X. wrote the manuscript. X.F. and X.X. assisted with the *in vivo* experiments. J.L. and W.Y. helped in nanoparticle preparation. H.Y. helped in mRNA synthesis. Y.L. helped with cryo-TEM sample preparation.

DECLARATION OF INTERESTS

There are no conflicts of interest to disclose.

REFERENCES

1. Noetzli, L.J., French, S.L., and Machlus, K.R. (2019). New insights into the differentiation of megakaryocytes from hematopoietic progenitors. Arterioscler. Thromb. Vasc. Biol. *39*, 1288–1300. https://doi.org/10.1161/atvbaha.119.312129.

2. Miyakawa, Y., Oda, A., Druker, B.J., Miyazaki, H., Handa, M., Ohashi, H., and Ikeda, Y. (1996). Thrombopoietin induces tyrosine phosphorylation of STAT3 and STAT5 in human blood platelets. Blood *87*, 439–446. https://doi.org/10.1182/blood.v87.2.439.bloodjournal872439.

3. Li, J., Xia, Y., and Kuter, D.J. (1999). Interaction of thrombopoietin with the platelet c-mpl receptor in plasma: binding, internalization, stability and pharmacokinetics. Br. J. Haematol. *106*, 345–356. https://doi.org/10.1046/j.1365-2141.1999.01571.x.

4. Emmons, R.V., Reid, D.M., Cohen, R.L., Meng, G., Young, N.S., Dunbar, C.E., and Shulman, N.R. (1996). Human thrombopoietin levels are high when thrombocytopenia is due to megakaryocyte deficiency and low when due to increased platelet destruction. Blood *87*, 4068–4071. https://doi.org/10.1182/blood.v87.10.4068.bloodjournal87104068.

5. Fanucchi, M., Glaspy, J., Crawford, J., Garst, J., Figlin, R., Sheridan, W., Menchaca, D., Tomita, D., Ozer, H., and Harker, L. (1997). Effects of polyethylene glycol-conjugated recombinant human megakaryocyte growth and development factor on platelet counts after chemotherapy for lung cancer. N. Engl. J. Med. *336*, 404–409. https://doi.org/10.1056/nejm199702063360603.

6. Nomura, S., Dan, K., Hotta, T., Fujimura, K., and Ikeda, Y. (2002). Effects of pegylated recombinant human megakaryocyte growth and development factor in patients with idiopathic thrombocytopenic purpura. Blood *100*, 728–730. https://doi.org/10.1182/blood.v100.2.728.

7. Li, J., Yang, C., Xia, Y., Bertino, A., Glaspy, J., Roberts, M., and Kuter, D.J. (2001). Thrombocytopenia caused by the development of antibodies to thrombopoietin. Blood *98*, 3241–3248. https://doi.org/10.1182/blood.v98.12.3241.

8. Kuter, D.J. (2007). New thrombopoietic growth factors. Blood *109*, 4607–4616. https://doi.org/10.1182/blood-2006-10-019315.

9. Kuter, D.J. (2009). Thrombopoietin and thrombopoietin mimetics in the treatment of thrombocytopenia. Annu. Rev. Med. *60*, 193–206. https://doi.org/10.1146/annurev.med.60.042307.181154.

10. Kuter, D.J., Rummel, M., Boccia, R., Macik, B.G., Pabinger, I., Selleslag, D., Rodeghiero, F., Chong, B.H., Wang, X., and Berger, D.P. (2010). Romiplostim or standard of care in patients with immune thrombocytopenia. N. Engl. J. Med. *363*, 1889–1899. https://doi.org/10.1056/NEJMoa1002625.

11. Cheng, G., Saleh, M.N., Marcher, C., Vasey, S., Mayer, B., Aivado, M., Arning, M., Stone, N.L., and Bussel, J.B. (2011). Eltrombopag for management of chronic immune

thrombocytopenia (raise): a 6-month, randomised, phase 3 study. Lancet *377*, 393–402. https://doi.org/10.1016/s0140-6736(10)60959-2.

12. Kuter, D.J., Bussel, J.B., Lyons, R.M., Pullarkat, V., Gernsheimer, T.B., Senecal, F.M., Aledort, L.M., George, J.N., Kessler, C.M., Sanz, M.A., et al. (2008). Efficacy of romiplostim in patients with chronic immune thrombocytopenic purpura: a double-blind randomised controlled trial. Lancet *371*, 395–403. https://doi.org/10.1016/S0140-6736(08)60203-2.

13. Polack, F.P., Thomas, S.J., Kitchin, N., Absalon, J., Gurtman, A., Lockhart, S., Perez, J.L., Pérez Marc, G., Moreira, E.D., Zerbini, C., et al. (2020). Safety and efficacy of the BNT162b2 mRNA Covid-19 vaccine. N. Engl. J. Med. *383*, 2603–2615. https://doi.org/10.1056/NEJMoa2034577.

14. Sahin, U., Karikó, K., and Türeci, Ö. (2014). mRNA-based therapeutics–developing a new class of drugs. Nat. Rev. Drug Discov. *13*, 759–780. https://doi.org/10.1038/nrd4278.

15. Thompson, M.G., Burgess, J.L., Naleway, A.L., Tyner, H., Yoon, S.K., Meece, J., Olsho, L.E.W., Caban-Martinez, A.J., Fowlkes, A.L., Lutrick, K., et al. (2021). Prevention and attenuation of Covid-19 with the BNT162b2 and mRNA-1273 vaccines. N. Engl. J. Med. *385*, 320–329. https://doi.org/10.1056/NEJMoa2107058.

16. Richner, J.M., Himansu, S., Dowd, K.A., Butler, S.L., Salazar, V., Fox, J.M., Julander, J.G., Tang, W.W., Shresta, S., Pierson, T.C., et al. (2017). Modified mRNA vaccines protect against zika virus infection. Cell *168*, 1114–1125.e10. https://doi.org/10.1016/j.cell.2017.03.016.

17. Meyer, M., Huang, E., Yuzhakov, O., Ramanathan, P., Ciaramella, G., and Bukreyev, A. (2018). Modified mRNA-based vaccines elicit robust immune responses and protect Guinea pigs from ebola virus disease. J. Infect. Dis. *217*, 451–455. https://doi.org/10.1093/infdis/jix592.

18. Heiser, A., Coleman, D., Dannull, J., Yancey, D., Maurice, M.A., Lallas, C.D., Dahm, P., Niedzwiecki, D., Gilboa, E., and Vieweg, J. (2002). Autologous dendritic cells transfected with prostate-specific antigen RNA stimulate CTL responses against metastatic prostate tumors. J. Clin. Invest. *109*, 409–417. https://doi.org/10.1172/jci0214364.

19. Rittig, S.M., Haentschel, M., Weimer, K.J., Heine, A., Muller, M.R., Brugger, W., Horger, M.S., Maksimovic, O., Stenzl, A., Hoerr, I., et al. (2011). Intradermal vaccinations with RNA coding for TAA generate CD8+ and CD4+ immune responses and induce clinical benefit in vaccinated patients. Mol. Ther. *19*, 990–999. https://doi.org/10.1038/mt.2010.289.

20. Zhang, H., You, X., Wang, X., Cui, L., Wang, Z., Xu, F., Li, M., Yang, Z., Liu, J., Huang, P., et al. (2021). Delivery of mRNA vaccine with a lipid-like material potentiates antitumor efficacy through toll-like receptor 4 signaling. Proc. Natl. Acad. Sci. USA *118*. https://doi.org/10.1073/pnas.2005191118.

21. Kormann, M.S.D., Hasenpusch, G., Aneja, M.K., Nica, G., Flemmer, A.W., Herber-Jonat, S., Huppmann, M., Mays, L.E., Illenyi, M., Schams, A., et al. (2011). Expression of therapeutic proteins after delivery of chemically modified mRNA in mice. Nat. Biotechnol. *29*, 154–157. https://doi.org/10.1038/nbt.1733.

22. Wang, Y., Su, H.-h., Yang, Y., Hu, Y., Zhang, L., Blancafort, P., and Huang, L. (2013). Systemic delivery of modified mRNA encoding herpes simplex virus 1 thymidine kinase for targeted cancer gene therapy. Mol. Ther. *21*, 358–367. https://doi.org/10.1038/mt.2012.250.

23. Karikó, K., Muramatsu, H., Keller, J.M., and Weissman, D. (2012). Increased erythropoiesis in mice injected with submicrogram quantities of pseudouridine-containing mRNA encoding erythropoietin. Mol. Ther. *20*, 948–953. https://doi.org/10.1038/mt.2012.7.

24. Yin, H., Song, C.Q., Dorkin, J.R., Zhu, L.J., Li, Y., Wu, Q., Park, A., Yang, J., Suresh, S., Bizhanova, A., et al. (2016). Therapeutic genome editing by combined viral and non-viral delivery of CRISPR system components *in vivo*. Nat. Biotechnol. *34*, 328–333. https://doi.org/10.1038/nbt.3471.

25. Wang, J., Exline, C.M., DeClercq, J.J., Llewellyn, G.N., Hayward, S.B., Li, P.W.L., Shivak, D.A., Surosky, R.T., Gregory, P.D., Holmes, M.C., and Cannon, P.M. (2015). Homology-driven genome editing in hematopoietic stem and progenitor cells using ZFN mRNA and AAV6 donors. Nat. Biotechnol. *33*, 1256–1263. https://doi.org/10.1038/nbt.3408.

26. Karikó, K., Buckstein, M., Ni, H., and Weissman, D. (2005). Suppression of RNA recognition by toll-like receptors: the impact of nucleoside modification and the evolutionary origin of RNA. Immunity *23*, 165–175. https://doi.org/10.1016/j.immuni.2005.06.008.

27. Jemielity, J., Fowler, T., Zuberek, J., Stepinski, J., Lewdorowicz, M., Niedzwiecka, A., Stolarski, R., Darzynkiewicz, E., and Rhoads, R.E. (2003). Novel "anti-reverse" cap analogs with superior translational properties. RNA *9*, 1108–1122. https://doi.org/10.1261/rna.5430403.

28. Karikó, K., Muramatsu, H., Welsh, F.A., Ludwig, J., Kato, H., Akira, S., and Weissman, D. (2008). Incorporation of pseudouridine into mRNA yields superior nonimmunogenic vector with increased translational capacity and biological stability. Mol. Ther. *16*, 1833–1840. https://doi.org/10.1038/mt.2008.200.

29. Anderson, B.R., Muramatsu, H., Nallagatla, S.R., Bevilacqua, P.C., Sansing, L.H., Weissman, D., and Karikó, K. (2010). Incorporation of pseudouridine into mRNA enhances translation by diminishing PKR activation. Nucleic Acids Res. *38*, 5884–5892. https://doi.org/10.1093/nar/gkq347.

30. Kauffman, K.J., Dorkin, J.R., Yang, J.H., Heartlein, M.W., DeRosa, F., Mir, F.F., Fenton, O.S., and Anderson, D.G. (2015). Optimization of lipid nanoparticle formulations for mRNA delivery *in vivo* with fractional factorial and definitive screening designs. Nano Lett. *15*, 7300–7306. https://doi.org/10.1021/acs.nanolett.5b02497.

31. Harrison, P., Robinson, M.S., Mackie, I.J., and Machin, S.J. (1997). Reticulated platelets. Platelets *8*, 379–383. https://doi.org/10.1080/09537109777050.

32. Lambert, M.P., and Gernsheimer, T.B. (2017). Clinical updates in adult immune thrombocytopenia. Blood *129*, 2829–2835. https://doi.org/10.1182/blood-2017-03-754119.

33. Morodomi, Y., Kanaji, S., Won, E., Ruggeri, Z.M., and Kanaji, T. (2020). Mechanisms of anti-GPIbα antibody-induced thrombocytopenia in mice. Blood *135*, 2292–2301. https://doi.org/10.1182/blood.2019003770.

34. Kuter, D.J., Mufti, G.J., Bain, B.J., Hasserjian, R.P., Davis, W., and Rutstein, M. (2009). Evaluation of bone marrow reticulin formation in chronic immune thrombocytopenia patients treated with romiplostim. Blood *114*, 3748–3756. https://doi.org/10.1182/blood-2009-05-224766.

35. Zufferey, A., Kapur, R., and Semple, J.W. (2017). Pathogenesis and therapeutic mechanisms in immune thrombocytopenia (ITP). J. Clin. Med. *6*, 16. https://doi.org/10.3390/jcm6020016.

36. Kuter, D.J. (2021). The treatment of immune thrombocytopenia (ITP)—focus on thrombopoietin receptor agonists. Ann. Blood *6*, 7. https://doi.org/10.21037/aob-21-23.

37. Bussel, J.B., Provan, D., Shamsi, T., Cheng, G., Psaila, B., Kovaleva, L., Salama, A., Jenkins, J.M., Roychowdhury, D., Mayer, B., et al. (2009). Effect of eltrombopag on platelet counts and bleeding during treatment of chronic idiopathic thrombocytopenic purpura: a randomised, double-blind, placebo-controlled trial. Lancet *373*, 641–648. https://doi.org/10.1016/s0140-6736(09)60402-5.

38. Cines, D.B., Gernsheimer, T., Wasser, J., Godeau, B., Provan, D., Lyons, R., Altomare, I., Wang, X., and Lopez, A. (2015). Integrated analysis of long-term safety in patients with chronic immune thrombocytopaenia (ITP) treated with the thrombopoietin (TPO) receptor agonist romiplostim. Int. J. Hematol. *102*, 259–270. https://doi.org/10.1007/s12185-015-1837-6.

39. McCarty, J.M., Sprugel, K.H., Fox, N.E., Sabath, D.E., and Kaushansky, K. (1995). Murine thrombopoietin mRNA levels are modulated by platelet count. Blood *86*, 3668–3675. https://doi.org/10.1182/blood.v86.10.3668.bloodjournal86103668.

40. Rizvi, F., Everton, E., Smith, A.R., Liu, H., Osota, E., Beattie, M., Tam, Y., Pardi, N., Weissman, D., and Gouon-Evans, V. (2021). Murine liver repair via transient activation of regenerative pathways in hepatocytes using lipid nanoparticle-complexed nucleoside-modified mRNA. Nat. Commun. *12*, 613. https://doi.org/10.1038/s41467-021-20903-3.

41. Karadagi, A., Cavedon, A.G., Zemack, H., Nowak, G., Eybye, M.E., Zhu, X., Guadagnin, E., White, R.A., Rice, L.M., Frassetto, A.L., et al. (2020). Systemic modified messenger RNA for replacement therapy in alpha 1-antitrypsin deficiency. Sci. Rep. *10*, 7052. https://doi.org/10.1038/s41598-020-64017-0.

42. Magadum, A., Kaur, K., and Zangi, L. (2019). mRNA-based protein replacement therapy for the heart. Mol. Ther. *27*, 785–793. https://doi.org/10.1016/j.ymthe.2018.11.018.

43. Trepotec, Z., Lichtenegger, E., Plank, C., Aneja, M.K., and Rudolph, C. (2019). Delivery of mRNA therapeutics for the treatment of hepatic diseases. Mol. Ther. *27*, 794–802. https://doi.org/10.1016/j.ymthe.2018.12.012.

44. Akinc, A., Querbes, W., De, S., Qin, J., Frank-Kamenetsky, M., Jayaprakash, K.N., Jayaraman, M., Rajeev, K.G., Cantley, W.L., Dorkin, J.R., et al. (2010). Targeted delivery of RNAi therapeutics with endogenous and exogenous ligand-based mechanisms. Mol. Ther. *18*, 1357–1364. https://doi.org/10.1038/mt.2010.85.

45. Kamaly, N., Yameen, B., Wu, J., and Farokhzad, O.C. (2016). Degradable controlled-release polymers and polymeric nanoparticles: mechanisms of controlling drug release. Chem. Rev. *116*, 2602–2663. https://doi.org/10.1021/acs.chemrev.5b00346.

46. Islam, M.A., Xu, Y., Tao, W., Ubellacker, J.M., Lim, M., Aum, D., Lee, G.Y., Zhou, K., Zope, H., Yu, M., et al. (2018). Restoration of tumour-growth suppression *in vivo* via systemic nanoparticle-mediated delivery of PTEN mRNA. Nat. Biomed. Eng. *2*, 850–864. https://doi.org/10.1038/s41551-018-0284-0.

47. Yan, R., Chen, M., Ma, N., Zhao, L., Cao, L., Zhang, Y., Zhang, J., Yu, Z., Wang, Z., Xia, L., et al. (2014). Glycoprotein Ibα clustering induces macrophage-mediated platelet clearance in the liver. Blood *124*, 466. https://doi.org/10.1182/blood.v124.21.466.466.

48. Chen, M., Yan, R., Dai, K., Zhou, K., Li, X., Zhang, Y., Liu, C., Jiang, M., Ye, H., Meng, X., et al. (2018). Akt-mediated platelet apoptosis and its therapeutic implications in immune thrombocytopenia. Proc. Natl. Acad. Sci. USA *115*, E10682–E10691. https://doi.org/10.1182/blood-2018-99-114952.

49. Chow, L., Aslam, R., Speck, E.R., Kim, M., Cridland, N., Webster, M.L., Chen, P., Sahib, K., Ni, H., Lazarus, A.H., et al. (2010). A murine model of severe immune thrombocytopenia is induced by antibody- and CD8+ T cell-mediated responses that are differentially sensitive to therapy. Blood *115*, 1247–1253. https://doi.org/10.1182/blood-2009-09-244772.

50. Lu, J., Lu, G., Tan, S., Xia, J., Xiong, H., Yu, X., Qi, Q., Yu, X., Li, L., Yu, H., et al. (2020). A COVID-19 mRNA vaccine encoding SARS-CoV-2 virus-like particles induces a strong antiviral-like immune response in mice. Cell Res. *30*, 936–939. https://doi.org/10.1038/s41422-020-00392-7.